IOSR Journal Of Applied Physics (IOSR-JAP)
e-ISSN: 2278-4861.Volume 12, Issue 5 Ser. III (Sep. – Oct 2020), PP 01-09
www.Iosrjournals.Org

Experimental investigation of structure, morphology, and optical properties of silica-based nanophosphor derived from rice husk

C. Mbakaan
Department of Science Laboratory Technology(Physics section), Benue State Polytechnic, Ugbokolo, Benue State, Nigeria.

Abstract
Phosphors are materials that exhibit the phenomenon of luminescence. They emit light when excited by radiation such as ultraviolet (UV) light or electron beams. A nanophosphor is a phosphor having particles with particle sizes ranging from 1-100 nm and it exhibits striking properties. In this paper nanosilica which can serve as a nanophosphor has been synthesized from a waste material known as rice husk by simple chemical and thermal treatments. The produced sample shows an amorphous structure and has nanosized spherical morphology. The average size of the particles of the sample is 32.62 nm. The silica nanophosphor has a wide bandgap of 5.6 eV and can be excited by both far UV (275 nm) and near UV (365 nm) light sources. The photoluminescence spectrum shows blue light emission which is confirmed by the CIE chromaticity diagram. The chromaticity coordinates of the sample are (0.1718, 0.1668), and (0.1708, 0.1629) for emissions spectrum obtained under 275, and 365 nm excitation wavelengths respectively. Besides, the sample hasa color purity of 70.7, and 71.7 % under the excitation wavelengths of 275, and 365 nm respectively. The result indicates that the silica nanophosphor is suitable potential candidate for applications in white light-emitting diodes (WLEDs).

Keywords: *Nanophosphor; silica; rice husk; amorphous; blue-light emission;morphology.*

Date of Submission: 30-09-2020 Date of Acceptance: 13-10-2020

I. Introduction

Nanoscience and nanotechnology a multidisciplinary field of research has gained much interest in all fields of study including studies on phosphors[1]. Phosphors are materials that exhibit the phenomenon of luminescence. Phosphor materials also known as luminescent materials produce visible color emission and are used for various applications including biomedical, solid-state lighting, and display applications [2,3]. A Phosphor having particles with particle sizes ranging from 1-100 nm is called a nanophosphor and it shows striking properties compared to their bulk counterpart. Nanophosphors have luminescent properties that are dependent on size, shape, crystal structure, and chemical environment [4]. Different types of nanophosphors have been developed in the past from different materials among these materials is silica whichcan be derived from different sources. Besides, silica-based materials have the potentials for use in a wide range of applications including photonics and biomedicine [5–8].

Silica-based phosphors have been produced using chemicals such as alkoxysilanes and polysiloxanes which are costly and difficult to obtained[5–14]. Today, interest is focused on the preparation of safe, environmentally friendly, chemically, and thermally stable phosphors [9,11,15]. Rice husk (RH) an inexpensive raw material is a suitable candidate material for producing safe and cheaper silica-based phosphors because it is made of a large amount of silica approximately 15-28 Wt %[7,13,16]. The silica from rice husk is produced at a controlled low temperature between 500-700 °C and is composed mainly of carbon (C), oxygen (O), and silicon (Si) [9,17]. Rice husk nanosilica (RHS) used as phosphors can be produced by adjusting suitable experimental conditions such as calcination temperature, time, and environment during synthesis [18]. Recently, different kinds of phosphors have been produced using silica derived from rice husk. White light-emitting nanophosphors developed from rice husk derived silica has been well investigated [2,7,9–11,13]. There are also some reports on green and red phosphors synthesized from silica derived from rice husk by doping with Mn^{2+} and rare earth (RE) ions respectively[4,19]. Though there are manyresearch studies on blue emission from silica, it is clear that studies on blue emission properties of silica-based nanophosphors derived from rice husk are uncommon.

In this paper, blue light-emitting nanosilica has been synthesizedfrom rice husk and structural, morphological, and optical properties have been well investigated.

II. Experimental

Rice husks (RHs) were collected from Makurdi rice mill in Benue State, Nigeria. Hydrochloric acid (37 wt%) was purchased from Sigma-Aldrich and was used as received without any further purification.

2.1 Preparation of nanosilica phosphor (silica nanophosphor) from RHs

About 80 g of raw rice husk was sieved and washed with deionized water to remove impurities. The husk was then dried in air for 24 hours and 50 g of the RHs were boiled in 100 mL of 10 wt% HCl for 2 hours. It wasthen washed with deionized water until a neutral pH of 7 was achieved. The acid pre-treated RHs were dried in an oven at 100 °C for 24 hours. The sample was then calcined in a box furnace at the temperature of 550 °C for 6 hours using a ramping rate of 10 °C/min. The produced nanosilica (nanophosphor) sample was allowed to cool overnight and it was stored for characterization.

The structure of the produced silica nanophosphor was determined by X-ray diffraction (XRD) using PANalytical X'Pert PRO with Cu Kα radiation (λ=0.15406 nm) while the morphology of the sample was obtained using Zeiss Auriga Field Emission Scanning Electron Microscope (FESEM) equipped with Energy-Dispersive X-ray (EDX) for chemical composition analysis and Jeol JEM-2100 Transmission Electron Microscope (TEM). The optical properties of the nanophosphor were determined using the PerkinElmer Lambda 1050 UV/Vis/ NIR spectrophotometer equipped with an integrated sphere at room temperature. Fourier transforms infrared (FTIR) spectra of the nanophosphor was obtained using the PerkinElmer ATR-FTIR 100 spectrometer. Photoluminescence (PL) measurements were done using an F-7000 spectrophotometer at room temperature.

III. Results and Discussion

3.1 X-ray diffraction analysis

Fig. 1 shows the XRD pattern of silica nanophosphor derived from rice husk. From Fig.1 it is clear that the sample exhibit a single broad peak from 15-30° with a maximum at 2θ approximately 22.19°, which signifies it is predominantly amorphous silica [20,21]. Besides there is a crystalline peak at 2θ =26.48° which is assigned to the 101 plane belonging to the quartz phase of silica.

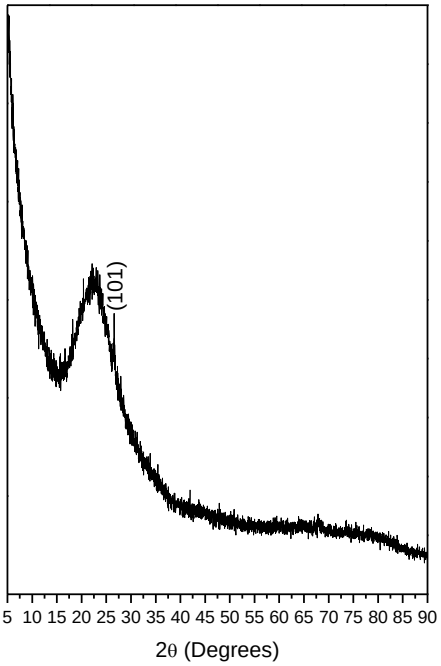

Fig.1 XRD pattern of silica nanophosphor derived from rice husk

3.2 Morphology and chemical composition

Fig.2 (a) is the SEM image of the silica nanophosphor sample. The SEM image displaysa high degree of agglomerated nano-size particles. The chemical composition of the sample was determined using EDX attached to SEM. The EDX of the sample is displayed in Fig. 2(b) which shows that the silica sample is composed of three major elements Carbon (C), oxygen (O), and silicon (Si). There is an impurity element Osmium(Os) which was not removed during acid pretreatment. The presence of these elements and their

distribution is also shown in the elemental mapping displayed in Fig. 2(c)-(g). The carbon impurity is intrinsic to the rice husk or maybe from the carbon tape used to hold the samples [4].

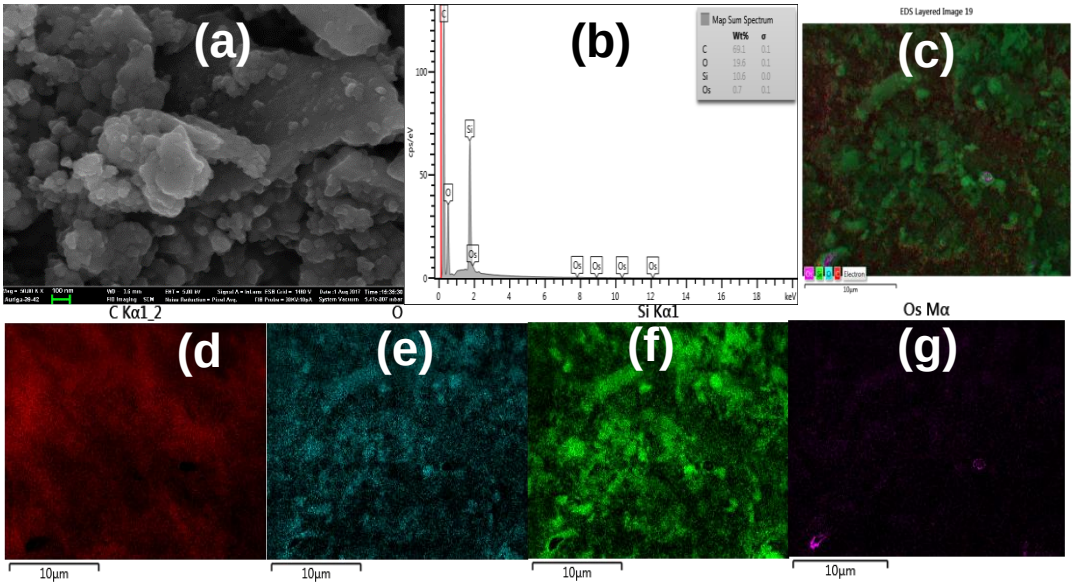

Fig. 2 (a) SEM image, (b) EDX spectrum, and (c)-(g) elemental mapping of rice husk derived nanosilica.

Fig. 3(a) displays the TEM micrograph of the silica nanophosphor sample. The TEM micrograph displays clusters of nanosized spherical particles. The particle size of the particles was determined from the TEM micrograph (Fig. 3a) and the result shows that the samples have particles with an average size of 32.62 nm. This result is also indicated in the histogram in Fig. 3(b).

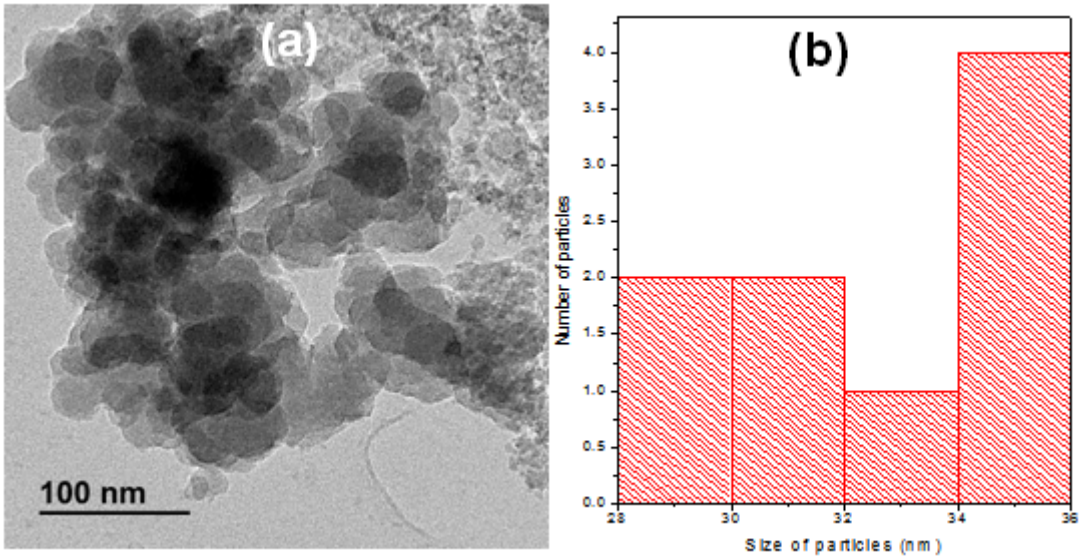

Fig. 3(a) TEM micrograph, and (b) histogram of silica nanophosphor derived from rice husk.

3.3 FTIR analysis

Fig. 4 presents the Fourier transform infrared (FTIR) spectrum of rice husk derived silica nanophosphor under investigation in this research. The spectrum shows two major absorption bands at 796 cm^{-1} and 1069 cm^{-1}. The absorption bands at 796 cm^{-1} and 1069 cm^{-1} are assigned to Si–O–Si symmetrical stretching vibrations and asymmetrical stretching mode of Si–O–Si respectively [4,22,23]. The absence of a major peak above 1600 cm^{-1}proves that there is no water content in the sample due to heat treatment. This result further proves the purity of the silica sample.

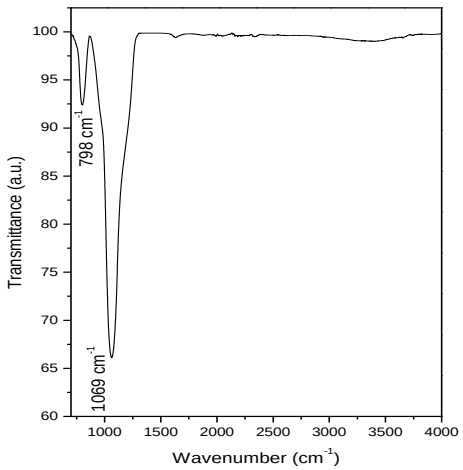

Fig. 4 FTIR spectra of silica nanophosphor derived from rice husk

3.4 Optical properties

3.4.1 Diffuse reflectance spectroscopy (DRS)

Diffuse reflectance spectroscopy is a very simple but very powerful spectroscopic tool for the determination of the bandgap energy (E_g) of powder samples[24]. This technique does not need the powder sample to be dispersed in liquid media such as methane, water, and ethanol, and so on. DRS requires the powder sample to be irradiated with light, and a portion of the light is regularly reflected at the powder surface and the remaining portion enters the powder and diffuses. This leads to the absorption of light of a particular wavelength by the sample and the measurement of the diffuse reflected light at different wavelengths produces a diffuse reflected spectrum. The intensity of the diffused reflected spectrum in the case of an infinitely thick sample is given by Kubelka-Munk (K-M) relation inequation 1[25].

$$\frac{k}{s}=\frac{(1-R_\infty)^n}{2R_\infty}=F(R_\infty) \qquad 1$$

Where $F(R_\infty)$ is proportional to the extinction coefficient, k is the absorption coefficient, s is the scattering coefficient which varies with particle size, and R_∞ is the diffuse reflectance or absolute diffuse reflectance of the sample defined by equation 2.

$$R_\infty=\frac{R_{sample}}{R_{reference}} \qquad 2$$

Most authors usually use the Kubelka – Munk (K-M) equation 3.

$$F(R)=\frac{(1-\mathrm{R})^2}{2R} \qquad 3$$

Where R is the reflectance; $F(R_\infty)$or $F(R)$ is proportional to the extinction coefficient α .

The bandgap is estimated by combining K-M equation 1 or 3 and Tauc equation 4by substituting α by $F(R_\infty)$ into the Tauc equation to give equation 5 and 6.

$$\alpha h\nu=A(h\nu-\mathrm{E_g})^n \qquad 4$$

$$[F(R_\infty)h\nu]=A(h\nu-\mathrm{E_g})^n \qquad 5$$

$$[F(R_\infty)h\nu]^{1/n}=A(h\nu-\mathrm{E_g}) \qquad 6$$

The bandgap (eV) of the material is obtained by plotting $[F(R_\infty)h\nu]^{1/n}$ against $h\nu$ and extrapolating the linear fitted region$[F(R_\infty)h\nu]^{1/n}=0$. $h\nu$is photon energy and h is Planck's constant while ν is the light

frequency (s^{-1}). The function $\left[F\left(R_\infty\right)h\nu\right]^{1/n}$ is known as the modified K-M function. Based on this function, n=2 for an indirect allowed transition and is plotted as $\left[F\left(R_\infty\right)h\nu\right]^{1/2}$ versus $h\nu$; n=3 for an indirect forbidden transition and is plotted as $\left[F\left(R_\infty\right)h\nu\right]^{1/3}$ versus $h\nu$; n=1/2 for a direct allowed transition and is plotted as $\left[F\left(R_\infty\right)h\nu\right]^2$ versus $h\nu$, and n=3/2 for a direct forbidden transition is plotted as $\left[F\left(R_\infty\right)h\nu\right]^{2/3}$ versus $h\nu$. Some authors usually exclude the $h\nu$ factor in the modified K-M function; this may have very little effect on the E_g value. By calculation;

$$E_g = \frac{1240 \times m}{-b} \qquad 7$$

Where E_g is calculated in eV, $-b$ and m are obtained by the linear fit $y = mx + b$ on the flat section of the diffuse reflectance spectrum [26–28].

Fig. 5 (a) displays the diffuse reflectance spectrum of silica nanophosphor in this research. It can be seen that the spectrum has absorption bands located at 204, 242, 320, and 380 nm. The absorption band located at 204 nm is assigned to near band absorption while 242, 320, and 380 nm are defect-related bands. Typically, this kind of defects in the silica network is associated with non-bridging oxygen hole centers (NBOHC), etc. [8,29].

The energy bandgap of the sample is determined from the Kubelka-Munk and Tauc relation in equation 5. The energy bandgap is determined from the point on the energy axis where the extrapolated linear portion of the graph is such that [F(R)hv] = 0. As can be seen in Fig. 5 (b), the energy bandgap of the sample is 5.6 eV.

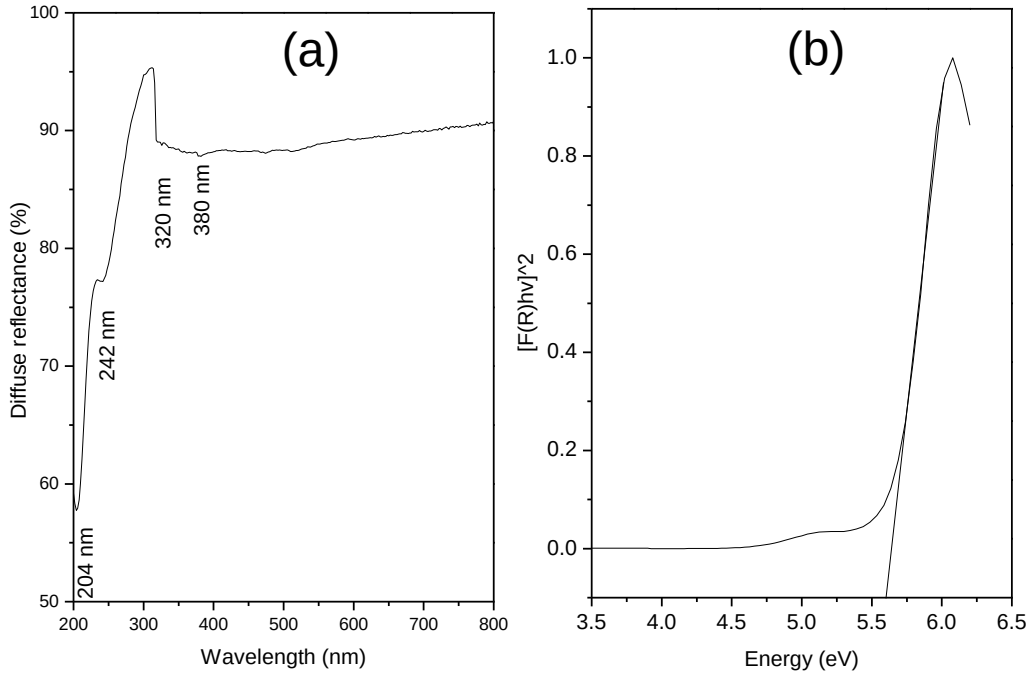

Fig. 5 (a) Diffuse reflectance spectrum, and (b) Energy bandgap of silica nanophosphor derived from rice husk.

3.4.2 Photoluminescence spectroscopy

Photoluminescence spectroscopy is a contactless, nondestructive method of probing the electronic structure of materials. In photoluminescence spectroscopy, light is directed onto a sample where it is absorbed and imparts excess energy into the material in a process known as photo-excitation [30]. The sample dissipates the excess energy in the form of emission of light generally known as photoluminescence. Photo-excitation makes electrons within a material to go into permissible excited states. By returning to the ground state, the electrons released the excess energy, which may include the emission of light through a radiative process [31,32]. In some cases, the electrons may return to the ground state through a nonradiative process. The energy of the emitted light (Photoluminescence) relates to the difference in energy levels between the two-electron

states, which are involved in the transition between the excited state and the equilibrium state. Besides the detection of light emission patterns, photoluminescence spectroscopy is employed to determine the bandgap of materials, detect the impurity levels and defects in materials, detect recombination mechanisms, and study surface structure and excited states.

In general, two processes are involved in the photoluminescence of phosphors; excitation and emission. An excitation spectrum is considered the product of an absorption spectrum and a plot of the quantum yield as a function of the wavelength. Excitation spectra are similar to absorption spectra but there is no direct relationship such that their relative intensities may be different and there may be additional peaks or missing peaks in the corresponding absorption spectra. Transitions observed in the excitation spectrum are the only ones that are efficient in populating the emitting level and generating luminescence. The absence of an energy level in the excitation spectrum when it is available in an absorption spectrum is an indication that it is not efficient enough to populate the emitting level. Besides, an excitation spectrum shows energy levels of the emitting ion, the sensitizing ion, or the antenna ligand. The excitation spectrum is used to determine the optimum excitation wavelength. Thus, the excitation wavelength required for measuring the luminescence (emission) spectrum is usually fixed at the most intense peak or the maximum of the most intense band in the excitation spectrum under consideration. The excitation spectrum also serves as a tool to reveal the presence of non-radiative transitions between levels. The emission spectrum reveals the presence of radiative transitions [33].

Fig. 6 (a) shows the photoluminescence excitation spectrum of the silica nanophosphors. The spectrum was obtained by monitoring emission at a wavelength of 435 nm. It can be observed that the spectrum shows two major excitation peaks with maxima located at 275 and 365 nm. These peaks are due to the presence of defects in the silica sample. Fig. 6(b) displays the emission spectrum of the sample obtained under the excitation wavelength of 275 and 365 nm. The emission spectrum in Fig.6 (b) is broad indicating an overlap of several emission bands. To identify the peaks, a Gaussian multiple peak fit (see Fig. 6c) was done using the spectrum obtained under the excitation wavelength of 365 nm and it shows six major bands with centers located at 402 (a), 412 (b), 427 (c), 446 (d), 472 (e), and 507 nm (f). The emission bands located at 402, 412, 427, and 446 nm are due to defects such as oxygen vacancies and non-bridging oxygen hole centers (NBOHC) while the emission bands at 472, and 507nmmay be due to carbon impurities [2,4,34,35]. The spectra of the sample showthe high intensity and large bandwidth when excited under 275 nm in the far-ultraviolet (UV) regionthan when excited in the near UV region (365 nm) of the electromagnetic spectrum.

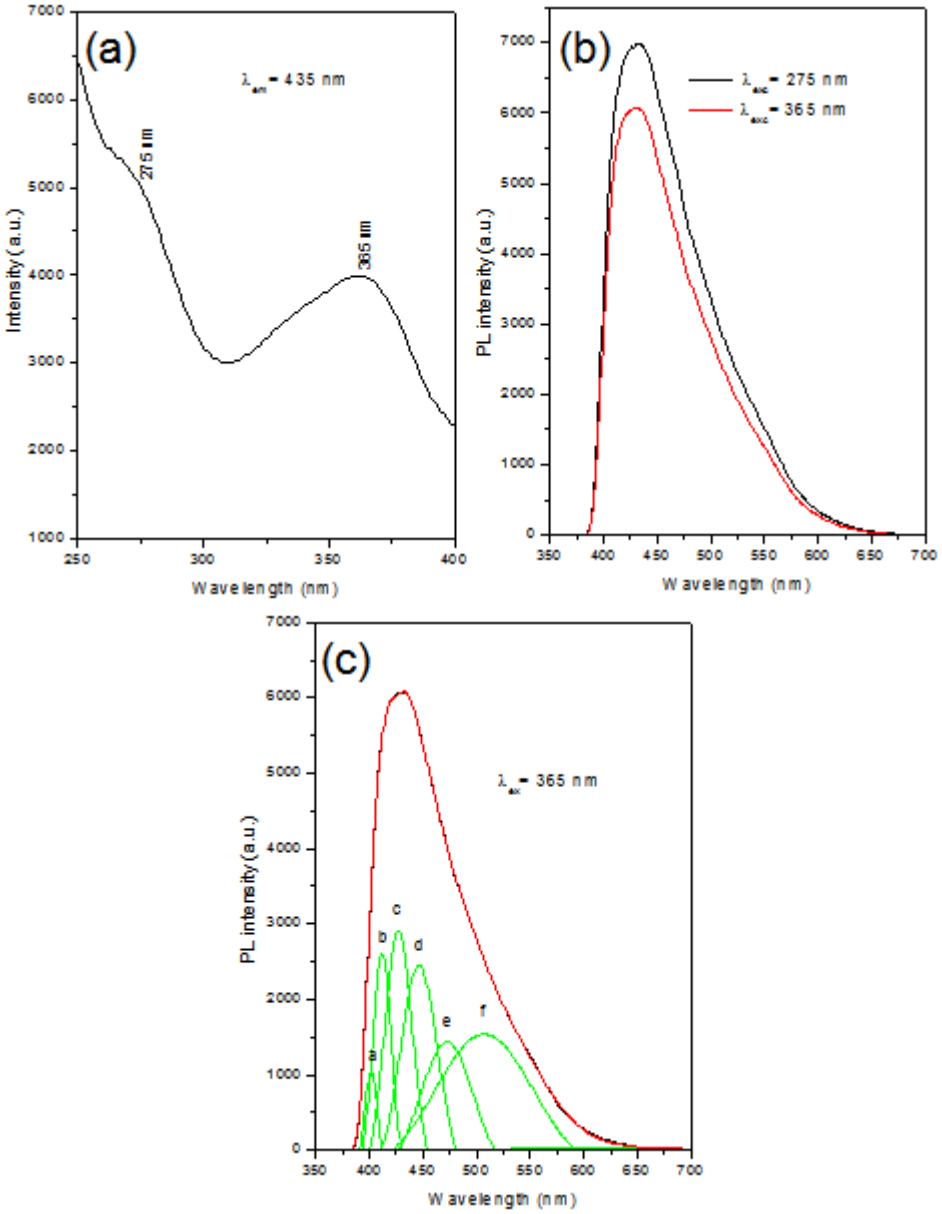

Fig.6 (a) PL excitation spectrum (b) PL (emission) spectrum, and (c) Gaussian fit of silica nanophosphor derived from rice husk.

3.4.3 Commission international de l'e'clairage (CIE) system

Fig.7 shows the CIE chromaticity coordinate diagram of the silica nanophosphor and it displays the emission color of the sample. The CIE coordinates (x, y) of the sample under 275, and 365 nm excitation wavelengths are (0.1718, 0.1668), and (0.1708, 0.1629) respectively, which indicates blue light emission. The color purity of the sample was calculated using equation 8 and the result shows that the sample has color purity of 70.7 % under an excitation wavelength of 275 nm and 71.7 % under the excitation wavelength of 365 nm.

$$color\ purity = \frac{\sqrt{(x_s - x_i)^2 - (y_s - y_i)^2}}{\sqrt{(x_d - x_i)^2 - (y_d - y_i)^2}} \times 100\% \qquad 8$$

where $(x_{s,}\ y_s)$, $(x_{d,}\ y_d)$ and $(x_{i,}\ y_i)$ are the color coordinates of the samples, dominant wavelength, and the CIE equal-energy illuminate, respectively. The result shows that Silica nanophosphors derived from rice husk could serve as a potential blue phosphor candidate for the near-UV white light-emitting diodes (WLEDs).

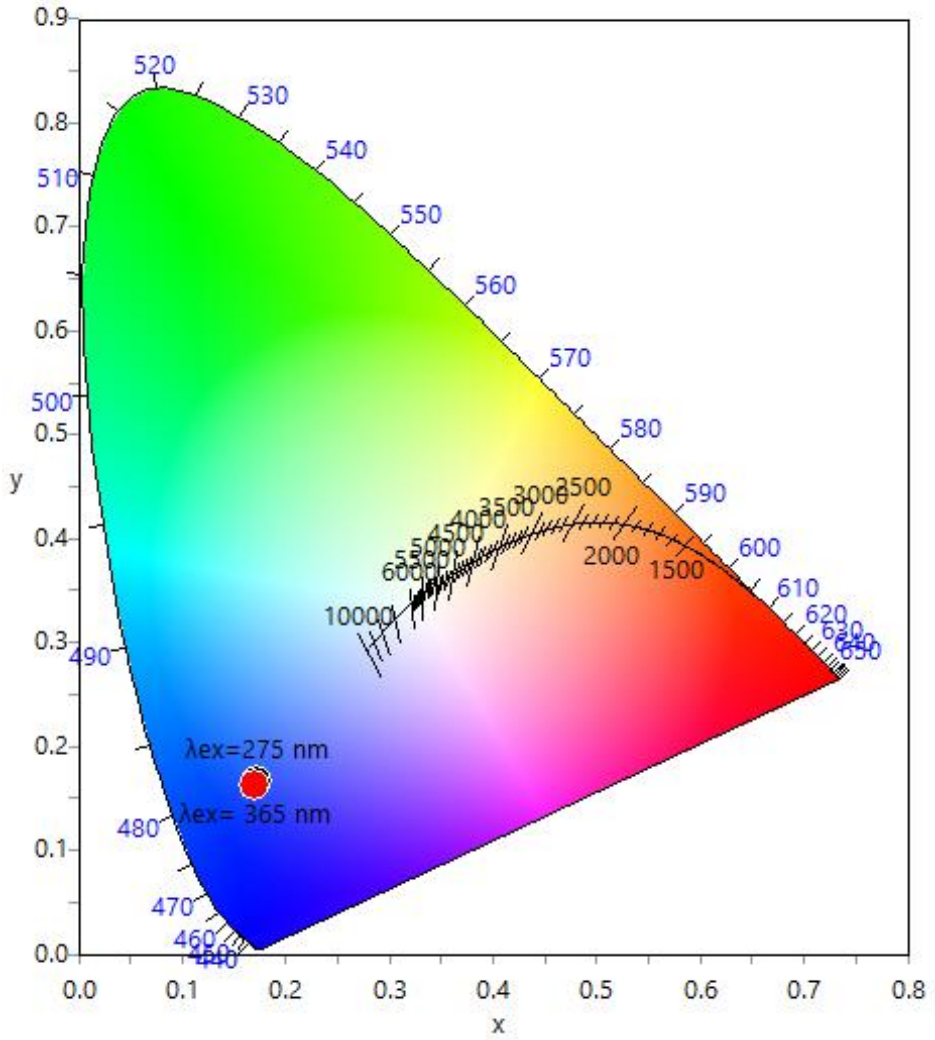

Fig.7 CIE chromaticity diagram of silica nanophosphor derived from rice husk

IV. Conclusion

Rice husk a waste material has been successfully used as a precursor to produce a blue-light-emitting nanophosphor by simple chemical and thermal treatments. The nanosilica particles which are predominantly amorphous in structure have nanosized spherical morphology. The average particle size of the particles of the silica nanophosphors is 32.62 nm. The sample has a wide bandgap of 5.6 eV and can be excited by far UV (275 nm) and near UV (365 nm) light sources. The photoluminescence spectrum shows emission in the blue and the CIE coordinate diagram shows chromaticity coordinates (0.1718, 0.1668), and (0.1708, 0.1629) for emissions spectrum obtained under 275, and 365 nm excitation wavelengths respectively. The result indicates that silica nanophosphor may be a suitable candidate for applications in WLEDs.

Acknowledgment

I express my gratitude to the Tertiary Education Trust fund (TETFUND), Abuja, Nigeria for sponsoring this research work.

Disclosures

The author declares no conflict of interest.

References

[1]. H. Chang, S.Q. Sun, Silicon nanoparticles: Preparation, properties, and applications, Chinese Phys. B. 23 (2014) 1–14. https://doi.org/10.1088/1674-1056/23/8/088102.

[2]. C. Mbakaan, I. Ahemen, A.N. Amah, A.D. Onojah, L. Koao, White-light-emitting Dy^{3+}-doped amorphous SiO<inf>2</inf> nanophosphors derived from rice husk, Appl. Phys. A Mater. Sci. Process. 124 (2018). https://doi.org/10.1007/s00339-018-2156-6.

[3]. R.S. A. Birkel, K.A. Danault, N.C. George, Advanced Inorganic Materials for Solid-State Lighting, in: Funct. Inorg. Mater. From Precursors to Appl., 2012: pp. 22–25.

[4]. C. Mbakaan, I. Ahemen, A.D. Onojah, A.N. Amah, K.G. Tshabalala, F.B. Dejene, Luminescent properties of Eu 3 + -doped silica

nanophosphors derived from rice husk, Opt. Mater. (Amst). 108 (2020) 110168. https://doi.org/10.1016/j.optmat.2020.110168.
[5]. M. Bardosova, M.E. Pemble, I.M. Povey, R.H. Tredgold, The Langmuir-Blodgett approach to making colloidal photonic crystals from silica spheres., Adv. Mater. 22 (2010) 3104–3124. https://doi.org/10.1002/adma.200903708.
[6]. S.S. Nobre, X. Cattoën, R.A.S. Ferreira, M.W.C. Man, L.D. Carlos, Efficient spectrally dynamic blue-to-green emission of bipyridine-based bridged silsesquioxanes for solid-state lighting, Phys. Status Solidi - Rapid Res. Lett. 4 (2010) 55–57. https://doi.org/10.1002/pssr.200903396.
[7]. Y. Liu, Z. Wang, H. Zeng, C. Chen, J. Liu, L. Sun, W. Wang, Photoluminescent mesoporous carbon-doped silica from rice husks, Mater. Lett. 142 (2015) 280–282. https://doi.org/10.1016/j.matlet.2014.12.034.
[8]. C. Zhang, J. Lin, Defect-related luminescent materials: Synthesis, emission properties, and applications, Chem. Soc. Rev. 41 (2012) 7938–7961. https://doi.org/10.1039/c2cs35215j.
[9]. Y. Ishikawa, S. Kawasaki, Y. Ishi, K. Sato, A. Matsumura, White photoluminescence from carbon-incorporated silica fabricated from rice husk, Jpn. J. Appl. Phys. 51 (2012). https://doi.org/10.1143/JJAP.51.01AK02.
[10]. H. Chen, Biogenic silica nanoparticles derived from rice husk biomass and their applications, Texas State University, 2013.
[11]. H. Chen, W. Wang, J.C. Martin, A.J. Oliphant, P.A. Doerr, J.F. Xu, K.M. DeBorn, C. Chen, L. Sun, Extraction of lignocellulose and synthesis of porous silica nanoparticles from rice husks: A comprehensive utilization of rice husk biomass, ACS Sustain. Chem. Eng. 1 (2013) 254–259. https://doi.org/10.1021/sc300115r.
[12]. Z. Wei, Z. Wang, W.R.T. Tait, M. Pokhrel, Y. Mao, J. Liu, L. Zhang, W. Wang, L. Sun, Synthesis of green phosphors from highly active amorphous silica derived from rice husks, J. Mater. Sci. 53 (2018) 1824–1832. https://doi.org/10.1007/s10853-017-1637-x.
[13]. Z. Wang, S. Zeng, Y. Li, W. Wang, Z. Zhang, H. Zeng, W. Wang, L. Sun, Luminescence Mechanism of Carbon-Incorporated Silica Nanoparticles Derived from Rice Husk Biomass, Ind. Eng. Chem. Res. 56 (2017) 5906–5912. https://doi.org/10.1021/acs.iecr.7b00700.
[14]. M. Narisawa, T. Kawai, S. Watase, K. Matsukawa, T. Dohmaru, Long-Lived Photoluminescence in Amorphous Si – O – C(– H) Ceramics Derived from Polysiloxanes, 6 (2012) 1–6. https://doi.org/10.1111/j.1551-2916.2012.05425.x.
[15]. A. Matsumura, Y. Ishii, K. Sato, Y. Ishikawa, S. Kawasaki, White light-emitting mesoporous carbon-silica nanocomposite, IOP Conf. Ser. Mater. Sci. Eng. 18 (2011) 5–9. https://doi.org/10.1088/1757-899X/18/10/102019.
[16]. W. Wang, J.C. Martin, X. Fan, A. Han, Z. Luo, L. Sun, Silica nanoparticles and frameworks from rice husk biomass, ACS Appl. Mater. Interfaces. 4 (2012) 977–981. https://doi.org/10.1021/am201619u.
[17]. Y. Ishikawa, Y. Ishii, K. Satoh, A. Matsumura, Preparation of light-emitting material by thermal treatment of Rice Husks, 102015 (n.d.). https://doi.org/10.1088/1757-899X/18/10/102015.
[18]. R. Bryant, R. Proctor, A. Hawkridge, M. Jackson, A. Yeater, K. Counce, P. Yan, W. McClung, A. Fjellstrom, Genetic variation and association mapping of silica concentration in rice hulls using a germplasm collection, Genetica. 139 (2011) 1383–1398. https://doi.org/10.1007/s10709-012-9637-x.
[19]. Z. Wei, Z. Wang, W.R.T. Tait, M. Pokhrel, Y. Mao, J. Liu, L. Zhang, W. Wang, L. Sun, Synthesis of green phosphors from highly active amorphous silica derived from rice husks, J. Mater. Sci. 53 (2018) 1824–1832. https://doi.org/10.1007/s10853-017-1637-x.
[20]. C. Lin, Y. Song, F. Gao, H. Zhang, Y. Sheng, K. Zheng, Z. Shi, X. Xu, H. Zou, Synthesis and luminescence properties of Eu(III)-doped silica nanorods based on the sol-gel process, J. Sol-Gel Sci. Technol. 69 (2014) 536–543. https://doi.org/10.1007/s10971-013-3254-8.
[21]. L. Gong, H. Zou, G. Wang, Y. Sun, Q. Huo, X. Xu, Y. Sheng, Synthesis and luminescence properties of monodisperse SiO 2 @ SiO 2 : Eu 3 + microspheres, 37 (2014) 583–588. https://doi.org/10.1016/j.optmat.2014.07.025.
[22]. Rachna Ahlawat, Synthesis, and Characterizations of Europium doped Silica Nanophosphor., Int. J. Adv. Res. Sci. Eng. 6 (2017) 1077–1085.
[23]. R. Al-oweini, H. El-rassy, Synthesis, and characterization by FTIR spectroscopy of silica aerogels prepared using several Si (OR) 4 and R 00 Si (OR 0) 3 precursors, J. Mol. Struct. 919 (2020) 140–145. https://doi.org/10.1016/j.molstruc.2008.08.025.
[24]. I. Ahemen, F.B. Dejene, Spectroscopic investigation of Ce 3 þ / Eu 3 þ co-doped Li 2 BaZrO 4 nanocrystalline phosphors, J. Alloys Compd. 735 (2018) 2436–2445. https://doi.org/10.1016/j.jallcom.2017.12.019.
[25]. Mohd Faizan and Shabbir Ahmad*, Structure and Luminescence Properties of Y2O3:Eu3+ Nanophosphors, J. At. Mol. Condens. Nano Phys. 3 (2016) 55–60.
[26]. R. López, R. Gómez, Band-gap energy estimation from diffuse reflectance measurements on sol-gel and commercial TiO2: A comparative study, J. Sol-Gel Sci. Technol. 61 (2012) 1–7. https://doi.org/10.1007/s10971-011-2582-9.
[27]. M. Nowak, B. Kauch, P. Szperlich, Determination of energy band gap of nanocrystalline SbSI using diffuse reflectance spectroscopy, Rev. Sci. Instrum. 80 (2009) 4–7. https://doi.org/10.1063/1.3103603.
[28]. P. Kubelka, New Contributions to the Optics of Intensely Light-Scattering Materials Part II: Nonhomogeneous Layers*, J. Opt. Soc. Am. 44 (1954) 330. https://doi.org/10.1364/JOSA.44.000330.
[29]. R. Salh, Defect Related Luminescence in Silicon Dioxide Network : A Review, in: Cryst. Silicon - Prop. Uses, InTech, 2011: pp. 135–172.
[30]. Y. Hong, W.Y. Lam, B. Zhong, Aggregation-induced emission : phenomenon, mechanism, and applications, R. Soc. Chem. (2009) 4332–4353. https://doi.org/10.1039/b904665h.
[31]. A.R. Barron, R. Ye, Photoluminescence Spectroscopy and its Applications, Connexions Modul. m38357 (2011) 1–11.
[32]. P. Packiyaraj, P. Thangadurai, Structural and photoluminescence studies of Eu 3 þ doped cubic Y 2 O 3 nanophosphors, J. Lumin. (2013) 1–7. https://doi.org/10.1016/j.jlumin.2013.07.074.
[33]. K. Binnemans, Interpretation of europium(III) spectra, Coord. Chem. Rev. 295 (2015) 1–45. https://doi.org/10.1016/j.ccr.2015.02.015.
[34]. L.F. Koao, H.C. Swart, R.I. Obed, F.B. Dejene, Synthesis and characterization of Ce3 doped silica (SiO 2) nanoparticles, J. Lumin. 131 (2011) 1249–1254. https://doi.org/10.1016/j.jlumin.2010.10.038.
[35]. A.E. Abbass, H.C.S.R.E. Kroon, White luminescence from sol-gel silica doped with silver, J. Sol-Gel Sci. Technol. (2015). https://doi.org/10.1007/s10971-015-3825-y.

C. Mbakaan. "Experimental investigation of structure, morphology, and optical properties of silica-based nanophosphor derived from rice husk." *IOSR Journal of Applied Physics (IOSR-JAP)*, 12(5), 2020, pp. 01-09.